Current Medicinal Chemistry, 2022, *29*, 1606-1621

RESEARCH ARTICLE

Feruloyl Sucrose Esters: Potent and Selective Inhibitors of α-glucosidase and α-amylase

Surabhi Devaraj[1], Yew Mun Yip[2], Parthasarathi Panda[1,3], Li Lin Ong[1,4], Pooi Wen Kathy Wong[1,4], Dawei Zhang[2], Yusuf Ali[5,*] and Zaher Judeh[1,*]

[1]School of Chemical and Biomedical Engineering, Nanyang Technological University, 62 Nanyang Drive, N1.2–B1-14, 637459, Singapore; [2]School of Physical and Mathematical Sciences, Nanyang Technological University, 21 Nanyang Link, 637371, Singapore; [3]Current Address: Dr. B.C. Roy College of Pharmacy & Allied Health Sciences, Dr. Meghnad Saha Sarani, Bidhan Nagar, Durgapur-713206, West Bengal, India; [4]Institute of Health Technologies, Interdisciplinary Graduate School, Nanyang Technological University, Singapore, 61 Nanyang Drive, ABN-02b-07, 637335, Singapore; [5]Lee Kong Chian School of Medicine, Nanyang Technological University, Singapore. 11a Mandalay Road, Clinical Sciences Building, 308232, Singapore

Abstract: ***Introduction*:** Feruloyl Sucrose Esters (FSEs) are a class of Phenylpropanoid Sucrose Esters (PSEs) widely distributed in plants. They were investigated as potential selective Alpha Glucosidase Inhibitors (AGIs) to eliminate the side effects associated with the current commercial AGIs. The latter effectively lowers blood glucose levels in diabetic patients but causes severe gastrointestinal side effects.

***Methods*:** Systematic structure-activity relationship (SAR) studies using *in silico, in vitro* and *in vivo* experiments were used to accomplish this aim. FSEs were evaluated for their *in vitro* inhibition of starch and oligosaccharide digesting enzymes α-glucosidase and α-amylase followed by *in silico* docking studies to identify the binding modes. A lead candidate, FSE **12** was investigated in an STZ mouse model.

***Results*:** All active FSEs showed desired higher % inhibition of α-glucosidase and desired lower inhibition of α-amylase in comparison to AGI gold standard acarbose. This suggests a greater selectivity of the FSEs towards α-glucosidase than α-amylase, which is proposed to eliminate the gastrointestinal side effects. From the *in vitro* studies, the position and number of the feruloyl substituents on the sucrose core, the aromatic 'OH' group, and the diisopropylidene bridges were key determinants of the % inhibition of α-glucosidase and α-amylase. In particular, the diisopropylidene bridges are critical for achieving inhibition selectivity. Molecular docking studies of the FSEs corroborates the *in vitro* results. The molecular docking studies further reveal that the presence of free aromatic 'OH' groups and the substitution at position 3 on the sucrose core are critical for the inhibition of both the enzymes. From the *in vitro* and molecular docking studies, FSE **12** was selected as a lead candidate for validation *in vivo*. The oral co-administration of FSE **12** with starch abrogated the increase in post-prandial glucose and significantly reduced blood glucose excursion in STZ-treated mice compared to control (starch only) mice.

***Conclusion*:** Our studies reveal the potential of FSEs as selective AGIs for the treatment of diabetes, with a hypothetical reduction of side effects associated with commercial AGIs.

ARTICLE HISTORY

Received: January 19, 2021
Revised: April 21, 2021
Accepted: April 26, 2021

DOI:
10.2174/0929867328666210827102456

Keywords: Diabetes mellitus, feruloyl sucrose esters, phenylpropanoid sucrose esters, natural products, α-glucosidase inhibition, α-amylase inhibition, glucose excursion.

*Address correspondence to these authors at the School of Chemical and Biomedical Engineering, Nanyang Technological University, 62 Nanyang Drive, N1.2–B1-14, Singapore 637459; Tel: +65-6790-6738; Fax: +65-6794-7553
Lee Kong Chian School of Medicine, Nanyang Technological University, Singapore. 11a Mandalay Road, Clinical Sciences Building, 308232, Singapore; E-mails: zaher@ntu.edu.sg; yusuf.ali@ntu.edu.sg

1875-533X/22 $65.00+.00

1. INTRODUCTION

Diabetes mellitus is an epidemic that plagues nearly 463 million people across the globe [1]. By 2030, WHO predicts that diabetes will be the seventh leading cause of death in the world [2]. The most common treatment for late-stage type-2 diabetes mellitus (T2D) is a long-acting formulation of insulin with increasing dosage [3]. However, there are many side effects associated with insulin, such as weight gain, lipodystrophy, hypoglycemia and life-threatening insulin shock [4]. Over time, patients receiving exogenous insulin may have exacerbated insulin resistance and they may develop allergies at the injection site. Oral drugs available for the treatment of T2D such as sulphonylureas, biguanides, meglitinides and thiazolidinediones also have numerous side effects which include but are not limited to weight gain, gastrointestinal disturbances, hypoglycemia, cardiac failure, respiratory tract infections, *etc*. [4-6].

Alpha-glucosidase inhibitors (AGIs) are a recent class of oral antidiabetics with obvious advantages in providing good overall control of postprandial rise in blood sugar and weight gain [7]. AGIs inhibit the major carbohydrate digesting enzymes, α-glucosidases and α-amylase, thereby reducing the amount of absorbed glucose from the intestine. α-amylase is present in saliva and duodenum and catalyzes the endohydrolysis of 1,4-α-D-glucosidic linkages in polysaccharide chains to produce simpler carbohydrates. On the other hand, α-Glucosidase enzymes are present in the brush border cells of the small intestine and they cleave the terminal non-reducing 1,4-linked α-D-glucose residues to release α-D-glucose units (exohydrolysis). The inhibition of these enzymes slows down the production of glucose in the gut lumen and limits its absorption into the bloodstream by the intestinal epithelial cells. Limiting the absorption of glucose helps to maintain normoglycemic levels in patients with impaired glucose tolerance. This leads to a decreased postprandial hyperglycemia (PPHG) and a better clinical outcome since high PPHG is linked to cardiovascular disorders, stroke, kidney disease and blindness [6, 8]. Commercial AGIs (acarbose, miglitol and voglibose) have been approved for the treatment of T2D. The gold standard acarbose has a significant effect on the reduction of PPHG and reduces the HbAlC level by 0.77% [5]. Most importantly, AGIs are not associated with the risk of life-threatening hypoglycemia. However, patient compliance and acceptance of AGIs are problematic since they cause severe gastrointestinal disturbances such as flatulence, diarrhoea, bloating and cramping [5, 9]. These side effects are attributed to the nonselective inhibition of the carbohydrate digesting enzymes by AGIs, leading to high inhibition of both α-glucosidase and α-amylase enzymes. High inhibition of α-amylase causes undigested longer-chain carbohydrates to pass into the lower section of the intestine, where fermentation by the gut microflora releases gases and other products causing these GI side effects [5, 10-12].

Recent developments of effective AGIs are centred on the isolation and screening of natural and synthetic lead compounds [13, 14]. However, it will be advantageous to develop selective AGIs with high inhibition of α-glucosidase and minimum inhibition of α-amylase to minimize the side effects of gastrointestinal disturbances for better patient acceptance and compliance.

Phenylpropanoid sucrose esters (PSEs) are natural compounds extracted from various plant species with reported biological activities [15]. PSEs showed inhibitory activities against both α-glucosidases and α-amylase [16, 17]. For example, lapathoside D**,** lapathoside C, hydropiperoside and vanicoside B (Fig. **1**) showed % α-glucosidase inhibition of 76.7±4.03, 24.8±1.92, 38.3±4.33, 23.8±6.53, respectively, (at a concentration of 225 μg/ml) in comparison to acarbose with 42.1±3.17 [17]. Diboside A (Fig. **1**) showed inhibitory activity against α-amylase with an IC_{50} of 26.9±0.6μM and sucrase (α-glucosidase enzyme) with an IC_{50} of 72±7 μM [18]. The corresponding values for acarbose were 14.2 ± 0.5 μM and 1.50 ± 0.08 μM, respectively. It is evident from these reports that PSEs exhibit α-glucosidase and α-amylase inhibitory activities and these activities are dependent on the type, number and position of the phenylpropanoid moieties. However, there lacks a systematic study on PSEs to identity lead compound(s) for further development as AGIs with high α-glucosidase inhibition and low α-amylase inhibition to markedly reduce gastrointestinal side effects while remaining efficacious for reducing PPHG.

Herein, feruloyl sucrose esters (FSEs), which are important phenylpropanoid sucrose esters (PSEs), will be investigated as selective AGIs capable of effectively controlling the rise in blood sugar and eliminating the gastrointestinal side effects associated with commercial AGIs. The structural features responsible for enhanced and selective enzyme inhibition will be revealed. Furthermore, the design of the diisopropylidene bridges and their impact on selectivity and inhibition will also be discussed. The effectiveness of FSE **12** in controlling PPHG in STZ-treated diabetic mice will be reported.

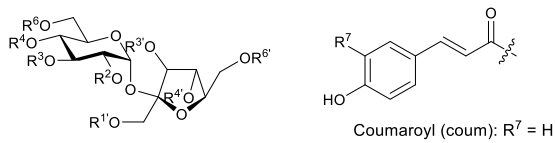

Coumaroyl (coum): R^7 = H
Feruloyl (feru): R^7 = OMe

Lapathoside D: $R^2 = R^3 = R^4 = R^6 = R^{1'} = H$, $R^{3'}$ = coum, $R^{4'} = H$, $R^{6'}$ = coum
Lapathoside C: $R^2 = R^3 = R^4 = H$, R^6 = feru, $R^{1'} = H$, $R^{3'}$ = coum, $R^{4'} = H$, $R^{6'}$ = coum
Hydropiperoside: $R^2 = R^3 = R^4 = R^6 = R^{1'}$ = coum, $R^{3'}$ = coum, $R^{4'} = H$, $R^{6'}$ = coum
Vanicoside B: $R^2 = R^3 = R^4 = H$, R^6 = feru, $R^{1'}$ = coum, $R^{3'}$ = coum, $R^{4'} = H$, $R^{6'}$ = coum
Diboside A: $R^2 = R^3 = R^4 = H$, R^6 = Coum, $R^{1'}$ = coum, $R^{3'}$ = coum, $R^{4'} = H$, $R^{6'}$ = Feru

Fig. (1). Structures of PSEs reported having α-glucosidases and α-amylase inhibitory activities.

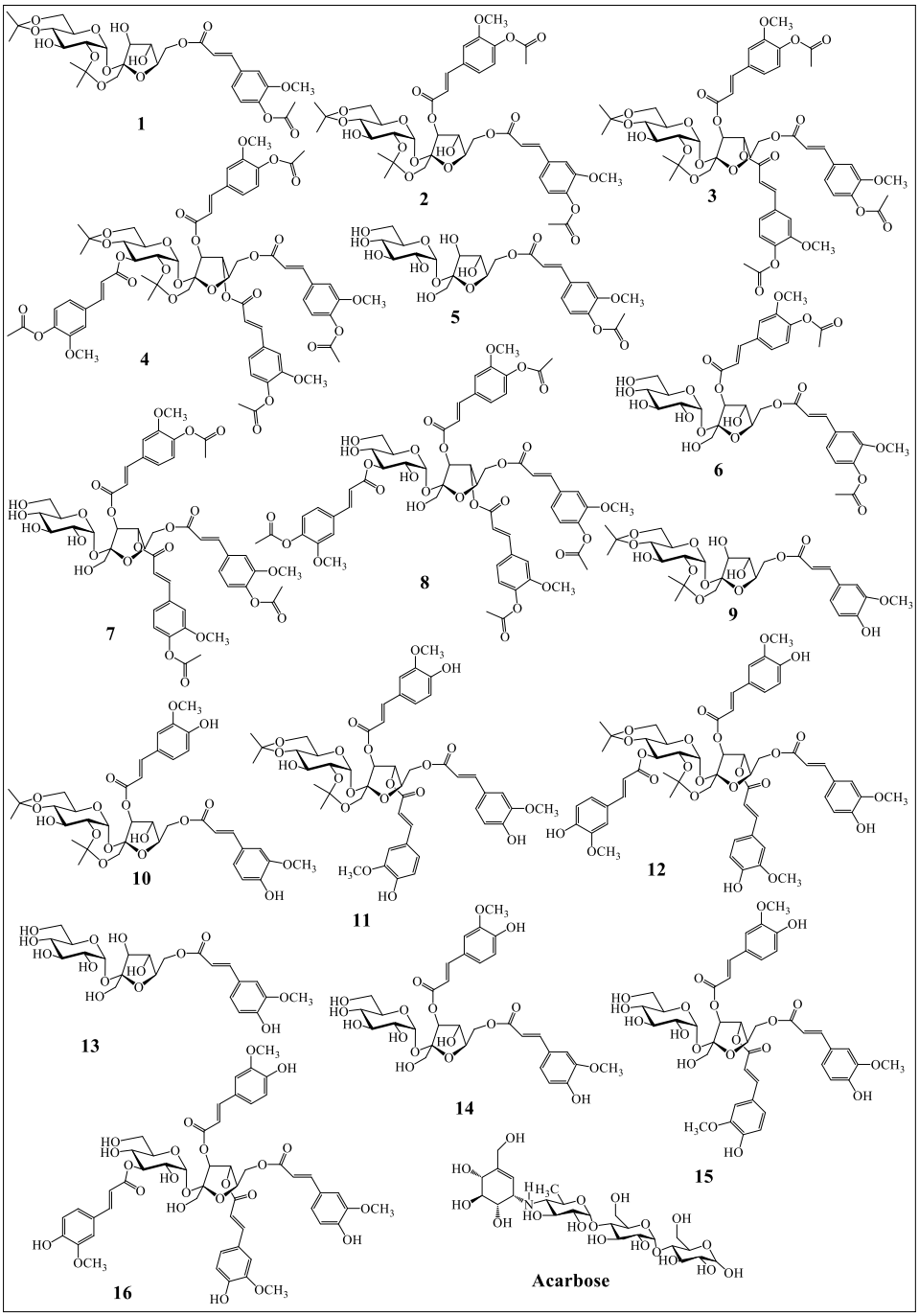

Fig. (2). Structures of the investigated FSEs **1**-**16** along with acarbose.

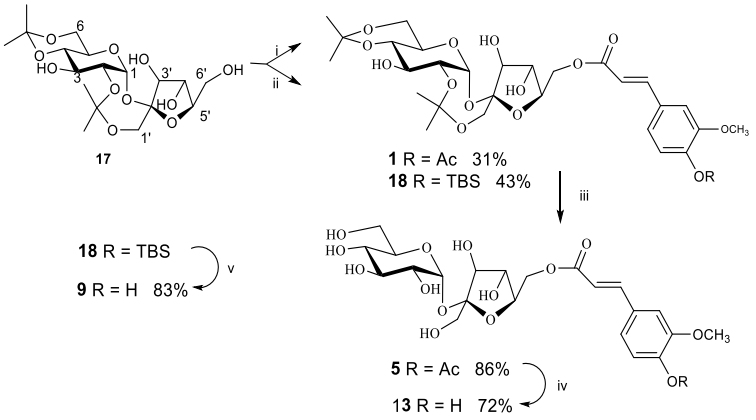

Reagents and conditions: i. *p*-Acetoxyferuloyl chloride (1.1 equiv.), dry pyridine, ice bath (4 °C) for 2 h then r.t. for 3 days; ii *p*-tert-Butyldimethylsilyloxy-3-methoxycinnamic acid (1.2 equiv), oxalyl chloride (1.3 equiv), DMF (0.2 equiv), pyridine (3.0 equiv), CH_2Cl_2, ice bath (4 °C), 14 h; iii. 60% aq. AcOH, 80 °C, 20 min.; iv.Piperidine, 95% EtOH, rt, 7 h; v. 1.56 3HF·NEt_3 (3.0 equiv), NEt_3 (2.0 equiv), pyridine, rt, 12 h.

Scheme 1. Synthesis of FSEs **5**, **9** and **13.**

2. RESULTS AND DISCUSSION

2.1. Design and Synthesis of the FSEs 1-16 Inhibitors

Since naturally occurring plant PSEs exhibited distinct variation in their enzymatic inhibition activities, analogues FSEs **1-16** were selected to establish an accurate structure activity relationship (Fig. **2**). The FSEs systematically differed in: (i) the number of feruloyl group(s) or degree of esterification on sucrose core, (ii) acyl-protected or free feruloyl aromatic OH groups and (iii) the presence or absence of diisopropylidene bridges on sucrose core to mainly control the degree of flexibility between the glucose and fructose moieties of sucrose. This wide structural diversity provides the opportunity to study several key structural features presumed to affect the inhibition selectivity and activity of the FSEs.

The synthesis of the FSEs **1-16** was previously reported (except FSEs **5**, **9** and **13**) by our group, using standard acylation protocols followed by selective removal of the protecting groups [18-20]. For a complete SAR in this study, FSEs **5**, **9** and **13** were synthesized as shown in Scheme 1. The reaction between the 2,1′:4,6-di-*O*-isopropylidene sucrose **17** and *p*-acetoxyferuloyl chloride gave the FSE **1** in 31% yield along with the undesired di-and tri- feruloyl compounds. PSE **1** was converted to FSE **5** in 86% yield by removal of the diisopropylidene bridges using 60% aq. acetic acid. Consequently, FSE **13** was obtained from FSE **5** in 72% yield by removal of the acetyl protection using piperidine. The reaction between sucrose **17** and the *in situ* generated *p-tert*-butyldimethylsilyloxy-3-methoxycinnamoyl chloride afforded the desired mono-feruloyl sucrose ester (FSE) **18** as the major product in 43% yield along with di- and tri-feruloyl sucrose esters. Consequently, removal of the TBS protecting group of FSE **18** was accomplished using HF. NEt_3 furnished the desired FSE **9** in 83% yield.

2.2. Structural Features of FSEs 1-16 Impact % Inhibition of α-glucosidase *In Vitro*

The FSEs **1-16** were screened for inhibition of α-glucosidase at the maximum solubility limit of 50 μg/ml with acarbose as the reference standard (Fig. **3**). The FSEs **1-16** exhibited variable % α-glucosidase inhibition values depending on their structures and ranged from no significant inhibition (NSA) to 98±4 % inhibition. The active FSEs showed a wide range of inhibition values where FSE **16** showed the highest inhibition value of 98±4%, which is > 3-fold that of acarbose (31±2%) (Fig. **3**). The mono-, di- and tri-feruloyl sucrose esters FSEs **1-3** and **5-7** having 1, 2 and 3 acyl-protected feruloyl moieties on the fructose ring, either with or without the diisopropylidene bridges, showed no significant activity (Fig. **3**). Similarly, mono-feruloyl sucrose esters **9** and **13** with free feruloyl aromatic OH, either with or without the diisopropylidene bridges, also showed no significant activities. However, acyl-protected tetra-feruloyl sucrose esters **4** and **8**, with an extra acyl-protected feruloyl moiety on the O-3 of the glucose ring, either with or without the diisopropylidene bridges, showed inhibition values of 46±4% and 35±10%, respectively (Fig. **3**). This result points to the importance of the O-3 feruloyl moiety for achieving α-glucosidase inhibition. In comparison to

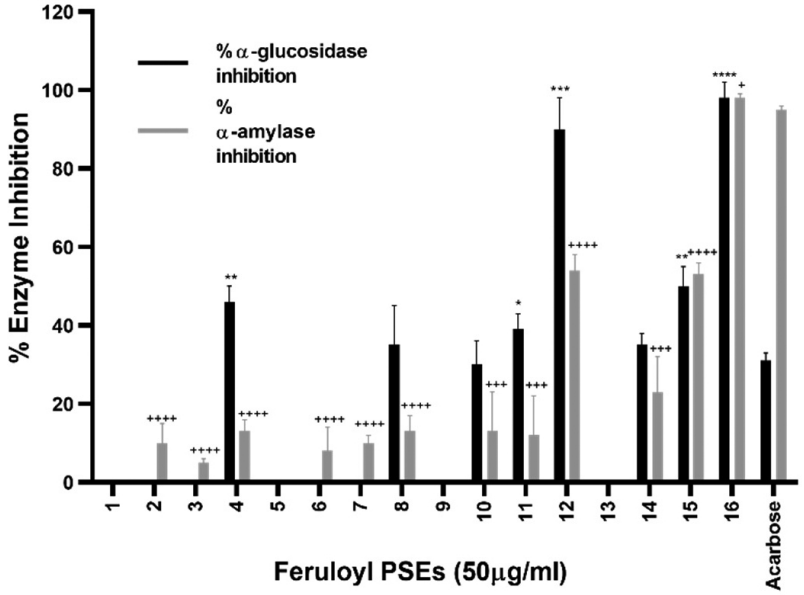

Fig. (3). Percentage inhibition of α-glucosidase and α-amylase by FSEs **1-16** with acarbose as the reference standard. Inhibition values are expressed as means ± SD; *n*=3. PSEs showing less than 5% enzyme inhibition are considered to have No Significant Activity (NSA). **p*≤0.05, ***p*≤0.01, ****p*≤0.001, *****p*≤0.0001 for significant change in α-glucosidase inhibition compared with acarbose; +*p*≤0.05, ++*p*≤0.01, +++*p*≤0.001, ++++*p*≤0.0001 for significant change in α-amylase inhibition compared with acarbose.

FSEs **1-3**, FSEs **10-12** with aromatic OH showed much higher inhibition values (Fig. **3**). Additionally, the increase in the inhibition values within FSEs **10-12** from 30±6% to 39±4% to 90±8% followed the increase in the number of feruloyl moieties having free aromatic OH from 2 to 3 to 4, respectively (Fig. **3**). This result highlights the importance of the free aromatic OH for inhibition. Likewise, a similar trend was observed when we compare FSEs **5-7** with FSEs **14-16,** confirming the importance of the aromatic OH for higher inhibition activity (Fig. **3**). As we compare FSEs **10-12** with FSEs **14-16**, the absence of the diisopropylidene bridges favor higher inhibitions activities (Fig. **3**). The SAR results show that the % inhibition brought by the feruloyl moieties (with or without acetyl protection) and the aromatic OH groups increases is in the following order: mono-feruloyl moieties < di-feruloyl < tri-feruloyl < tetra-feruloyl; 1 OH < 2 OH < 3 OH < 4 OH. Additionally, the SAR results show the absence of the diisopropylidene bridges increases the % inhibition activity. This trend is observed throughout (Fig. **3**).

The IC_{50} values for α-glucosidase inhibition were calculated for selected FSEs (Table **1**). FSEs **12**, **15** and **16** showed IC_{50} values of 4±2μM, 205±10μM, and 5±2μM, respectively, which are lower than that of acarbose with IC_{50} value of 328±7μM. Both FSEs **12** and **16** with four acyl-free feruloyl moieties showed similar IC_{50} values and are > 65 times lower than that of acarbose.

Table 1. IC_{50} values for α-glucosidase and α-amylase inhibition by FSEs 12, 15 and 16.

Entry	PSE	IC_{50} value (μM)	IC_{50} value (μM)
		α-Glucosidase	α-Amylase
1	**12**	4±2	N.D
2	**15**	205±10	N.D
3	**16**	5±2	2 ±1
4	Acarbose	328±7	5±0.1

IC_{50} values are expressed as means ± SD; *n*=3. N.D = not determined; IC_{50} values were calculated using GraphPad PRISM software.

2.3. Structural Features of FSEs 1-16 Impact % Inhibition of α-amylase *In Vitro*

Similarly, the FSEs **1-16** were tested for their inhibitory activity against α-amylase at the same concentration of 50 μg/ml with acarbose as the reference standard (Fig. **3**). Except for FSE **16**, all other FSEs showed much lower % inhibition of α-amylase in comparison to inhibition with acarbose. Additionally, the inhibition values significantly depended on the structural features of the FSEs. Mono-feruloyl sucrose esters **1**, **5**, **9** and **13** with only one feruloyl moiety showed no significant α-amylase inhibition irrespective of the presence or absence of the diisopropylidene bridges and if the feruloyl aromatic OH was free or acyl-protected (Fig. **3**). This

result agrees with the α-glucosidase inhibition values and confirms that mono-feruloyl moieties have no inhibition effects (Fig. **3**). However, as the number of the acetyl-protected feruloyl moieties increased to 2, 3 and 4, as in di-, tri-, and tetra-feruloyl sucrose esters **2-4** and **6-8**, the % inhibition activity increased gradually (except for FSE **3**), thus confirming the impact of the number of the feruloyl moieties on inhibition activity (Fig. **3**). Again, the presence (FSEs **2-4**) or absence (FSEs **6-8**) of the diisopropylidene bridges had little impact on the activity of these FSEs. FSEs **10-12** having free aromatic OH groups showed higher % α-amylase inhibition than the corresponding FSEs **2-4** with the acetyl-protected OH groups, thus confirming the role of free aromatic OH for higher inhibition, as observed in the case of α-glucosidase inhibition. The highest increase was observed in the case of FSE **12** with four free aromatic OH groups, which showed 54±4% inhibition (Fig. **3**). Again, FSEs **10-12** with the diisopropylidene bridges and free aromatic OH groups showed higher inhibition in comparison to FSEs **6-8** having no diisopropylidene bridges but with acetyl protection, further supporting the importance of free aromatic OH groups for higher inhibition (Fig. **3**). FSEs **14-16** with free aromatic OH groups also showed a similar trend in comparison to FSEs **6-8,** thus confirming the role of the free aromatic OH for higher inhibition. FSEs **14-16** without the diisopropylidene bridges showed higher inhibition activities (23±9, 53±3 and 98±1, respectively) in comparison to FSEs **10-12** with the diisopropylidene bridges (13±10, 12±10, 54±4, respectively). Again, the highest inhibition was observed for FSE **16** with four feruloyl aromatic OH groups (Fig. **3**). FSEs **14-16** with free aromatic OH groups also showed higher inhibition activities in comparison to FSEs **6-8** having acetyl protection groups (Fig. **3**). Similar to the case of α-glucosidase inhibition, the SAR studies showed the α-amylase inhibition correlates to the number of feruloyl moieties (with or without acetyl protection) and the number of free aromatic OH groups to be 4 > 3 > 2 > 1. Additionally, the presence of the diisopropylidene bridges decreases the inhibition activity values in the FSEs with free aromatic OH groups but has no significant effect on FSEs with acyl-protected aromatic OH groups. The IC_{50} value of FSE **16** at 2 ±1 μM was found to be 2.5 times higher than that of acarbose at 5±0.1 μM (Table **1**).

2.4. FSEs 10-12 and 14-16 Docked Close to the Active Site of α-glucosidase

Molecular docking studies of selected FSEs **10-12** and **14-16** were performed to determine their binding modes with α-glucosidase. These FSEs were specifically selected to demonstrate the impact of the structural factors (OH groups, number of feruloyl moieties and diisopropylidene bridges) on binding with the receptor sites and to understand if the binding results correlate with the observed inhibition activity values in Fig. (**3**). A homology model was built using yeast isomaltase (PDB ID 3A4A) since the protein structure of yeast α-glucosidase is unavailable. The binding modes (Fig. **4**) and the Ligand Interaction Diagrams (Fig. **5**) of the FSEs **10-12** and **14-16** show the site of docking as well as the amino acid residues that interact with these FSEs and help stabilize the complex (FSE-α-glucosidase). A colouring scheme has been employed to visualize the orientations of the feruloyl substituents at specific positions since certain binding trends remained common across all the FSEs. FSEs **10-12** and **14-16** did not dock into the active site of the enzyme but rather at one close to the active site (Fig. **4**). From the binding mode pictures, the sucrose core of di-feruloyl sucrose esters **10** and **14** projects into the binding pocket while the feruloyl moieties at O-3' (blue) and at O-6' (pink) extended at the periphery of the enzyme (Fig. **4**). In the case of the tri-feruloyl sucrose esters **11** and **15**, a similar trend was observed and the third feruloyl group at O-4' (purple) was also projected at the periphery (Fig. **4**). In tetra-feruloyl sucrose esters **12** and **16**, the fourth feruloyl at O-3 (yellow), and through a reorientation, projected towards the active site where glucose molecule was docked while the rest of the feruloyl moieties are seen to project at the periphery (Fig. **4**). Based on the docking modes, we speculate that the FSEs block the entry of the substrate into the active site, thus inhibiting the enzyme. This is similar to the inhibition of α-glucosidase reported by Yan and colleagues [21]. The ligand interaction diagrams of FSEs **12** and **16** were examined for comparison since both FSEs have similar structural features except that FSE **16** lacks the diisopropylidene bridges (Fig. **5**). Based on the ligand interaction diagram of FSE **12**, the aromatic OH of the feruloyl at O-3 forms a hydrogen bond with ARG442 while the carbonyl (C=O) of the feruloyl at O-3' forms a hydrogen bond with ASN242 (Fig. **5**). The aromatic moiety of O-3' is in particular, solvent-exposed. Additionally, four π-π stacking bonds are observed between the feruloyl aromatic rings with the residues PHE178, PHE158, PHE314 and ARG442 (Fig. **5**). In FSE **16**, the aromatic OH of the feruloyls at O-3 and O-3' form hydrogen bonds with ASP215 and GLU277, respectively, (Fig. **5**). The FSE **16** aromatic rings show five π-π stacking interactions with the HIS240, HIS246, HIS280, PHE158 and PHE303 residues (Fig. **5**). Unlike FSE **12**, FSE **16** is not highly solvent

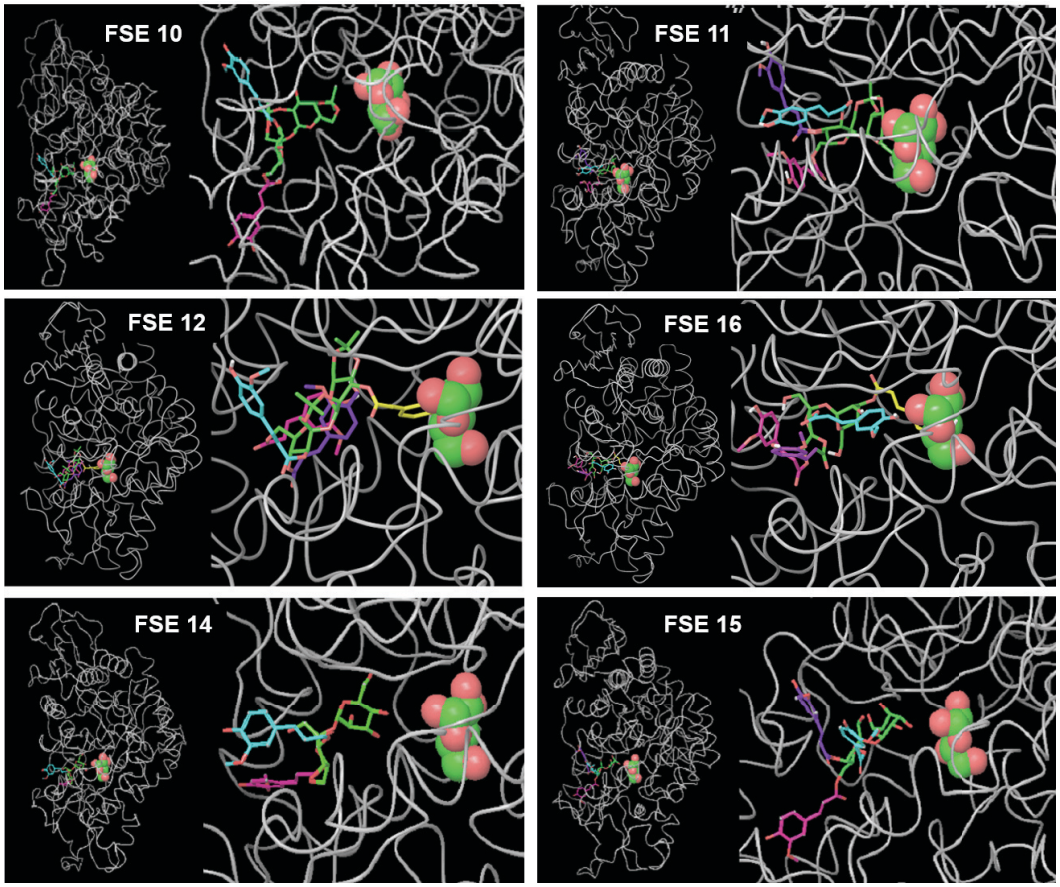

Fig. (4). Binding mode pictures for FSEs **10-12** and **14-16** docked with homology modelled yeast α-glucosidase; Legend: The coloring scheme in the binding mode pictures for docking with α-glucosidase is as follows: the sucrose core of the ligand (FSE) is colored in green; O-6' feruloyl is pink; O-4' feruloyl is purple; O-3' feruloyl is blue and O-3 is yellow. The enzyme is represented in 'ribbon style' and the active site shows a molecule of glucose docked in it in ball representation. The glucose molecule was shown in the active site to illustrate that the FSEs block the active site and therefore prevent the glucose molecule from entering the active site. Docking studies were done without the glucose molecule. *(A higher resolution / colour version of this figure is available in the electronic copy of the article).*

exposed. Due to the absence of the diisopropylidene bridges, FSE **16** posses more flexibility and steric freedom than FSE **12**. As a consequence, the molecule assumes better fitting conformation in the enzyme pocket resulting in additional weak π -π stacking interaction. The docking and ligand interaction diagram results correlated with the *in vitro* inhibition values for FSEs **16** and **12,** which showed inhibition of 98±4% and 90±8%, respectively. This slight difference in the % inhibition between these two FSEs is attributed to the additional weak *π-π* stacking interactions shown by FSE **16,** which is known to be much weaker than hydrogen bond interactions [22]. In this case, the diisopropylidene bridges between the fructose and glucose rings are flexible enough to allow both FSEs **12** and **16** to attain the most preferable confirmation for maximum interaction to achieve high inhibition values.

2.5. FSEs 12 and 14-16 Bind Preferentially at the Primary Active Sites of α-amylase and Docking is Greatly Affected by the Conformational Rigidity of the FSEs

α-Amylase has multiple inhibitory binding sites [18]. Therefore, molecular dynamics (MD) studies were performed to calculate the binding affinity of FSEs **12** and **14-16** inhibitors at the different binding sites (Fig. **6**). To do this, the lowest energy docked pose for FSEs **12** and **14-16** docked into α-amylase was used for MD calculations. The MMPBSA method was used to calculate the free energy of binding of the FSEs **12** and **14-16** at the primary as well as the two secondary sites SS1 and SS2 (Fig. **6**). All the FSEs **12** and **14-16** exhibited the lowest (most negative) free energy of binding at the primary binding site, thus confirming it to be the most preferred for binding. The differences in the free energy of binding at the primary site were

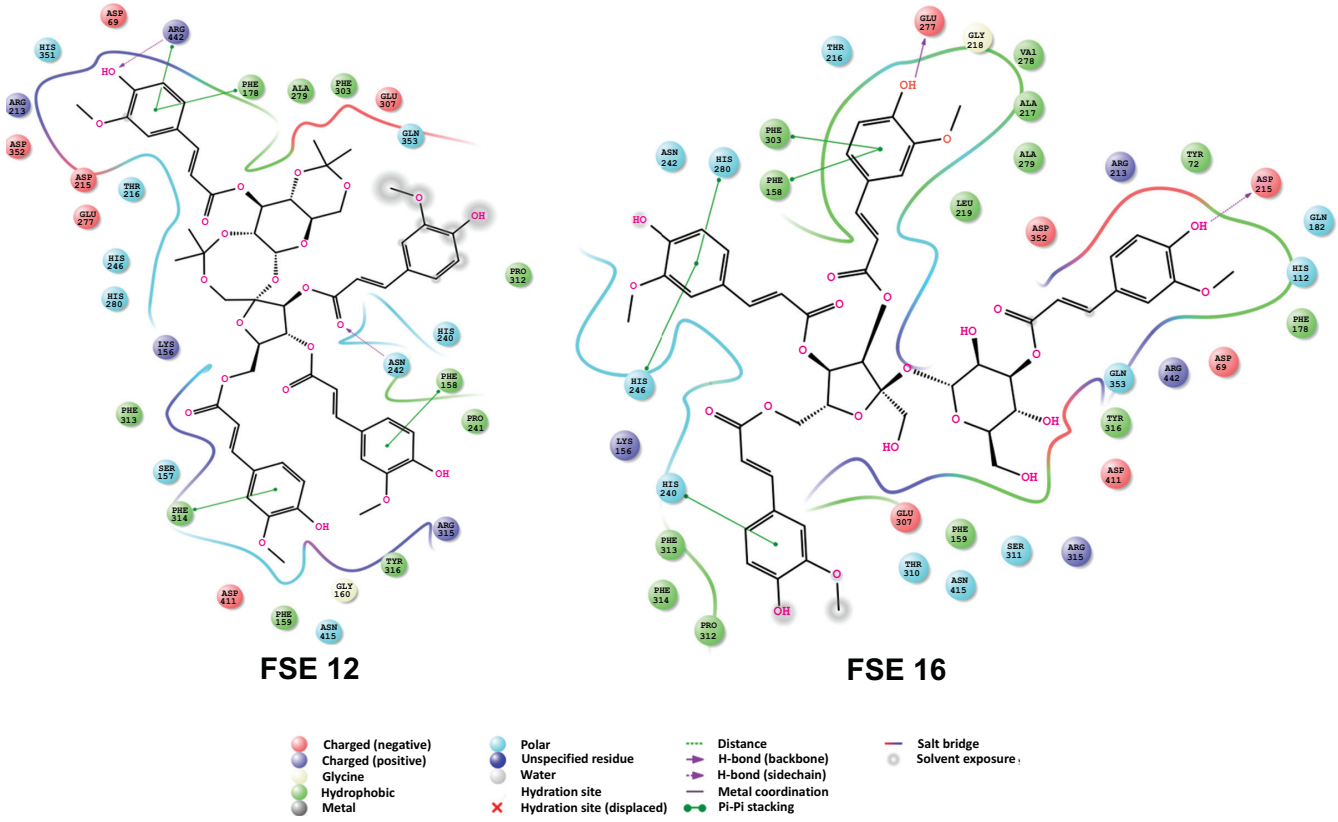

Fig. (5). Ligand Interaction Diagrams for the molecular docking top-scoring complexes between FSE **12** and FSE **16** with homology modelled yeast α-glucosidase. *(A higher resolution / colour version of this figure is available in the electronic copy of the article).*

more pronounced than at the secondary sites SS1 and SS2, whereas the differences in the energies between SS1 and SS2 were modest (Fig. **6**). The free energy of binding of FSEs **14-16** decreases as the number of feruloyl moieties increases from 2 to 3 to 4 with values being -7.41, -8.44 and -9.02 kcal/mol, respectively (Fig. **6**). The binding energy of the FSE **16,** which has no diisopropylidene bridges is lower than the corresponding FSE **12** with the diisopropylidene bridges (-9.02 kcal/mol *vs* -7.96 kcal/mol, Fig. **6**). The overall trend in binding energies for these FSEs is FSE **16 (**-9.02 kcal/mol) > FSE **15** (-8.44 kcal/mol) > FSE **12** (-7.96 kcal/mol) > FSE **14** (-7.41 kcal/mol), which is consistent with the trend in the *in vitro* % inhibition activities: FSE **16 (**98±1) > FSE **15** (53±3) > FSE **12** (54±4) > FSE **14** (23±9) (Fig. **1**). These results are also consistent with the results obtained from the docking studies (data in supporting information) and ligand inhibition diagrams (Fig. **7**). In the case of SS1 and SS2, the binding energies of FSEs **14-16** are higher than the primary site but follow a similar trend as that of the primary site except for FSE **15** whose binding energy deviates slightly from what is predicted.

The MD results are consistent with the *in vitro* experiments and support the conclusions that a higher number of feruloyl moieties and free OH groups as well as the absence of the diisopropylidene bridges increases the inhibition of α-amylase.

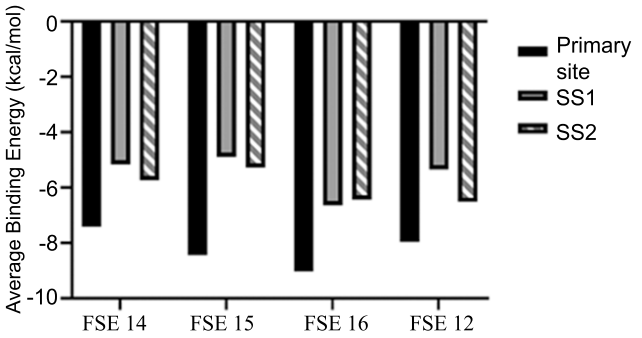

Fig. (6). Free energy of binding of FSEs **12** and **14-16** at the primary and secondary SS1 and SS2 sites.

Docking with porcine pancreatic α-amylase (PDB ID 1OSE) was performed using FSEs **12** and **14-16** to determine the binding modes and to examine whether the binding results correlate with the *in vitro* inhibition results and compare it with α-glucosidase docking. These FSEs were selected due to the differences in their structural features (Fig. **1**) and their *in vitro* inhibition values (Fig. **3**). Specifically, the remarkable difference in the *in vitro* inhibition activity between the two tetra-feruloyl sucrose esters - FSE **12** (54±4%) and FSE **16** (98±1%) is intriguing. Based on docking studies, five regions comprised key residues that form the active sites in α-amylase [23]. This seemed to agree with previous reports on the active site regions of porcine pancreatic α-amylase [23]. Interaction of the aromatic OH groups, feruloyl substituents, diisopropylidene bridges and/or sucrose core with these residues usually enhance the inhibition activity. In the binding mode pictures, the FSEs **12** and **14-16** are depicted in grey and the five regions containing the key residues in the active sites (residues 50-63; 145-151; 197-200; 233-240; 300-306) are highlighted in red (refer supporting information). The rest of the enzyme is depicted in blue. Binding mode pictures exhibited that the di- and tri-feruloyl sucrose esters **14** and **15** interact with and some of the residues in the active site. In the case of the tetra-FSE **16**, the sucrose core as well as all four feruloyl moieties are seen to interact with the residues in the active site. The ligand interactions diagrams of FSEs **12** and **14-16** are shown in Fig. (**7**). Di-FSE **14** exhibits two hydrogen bonding between its O-3' and O-6' feruloyl aromatic OH and ILE148 and ASP197, respectively. Additionally, its O-6' feruloyl moiety shows π-π stacking interactions with TYR62. Tri-FSE **15** displays one more additional hydrogen bonding between the O-4' feruloyl aromatic OH and ASN53 in addition to the hydrogen bonding that di-FSE **14** shows. The tetra-FSE **16** even shows more interactions with four hydrogen bonding between O-3, O-4' and O-6' feruloyl aromatic OH groups and water, ASN53 and ASP197, respectively, and between O-3 feruloyl aromatic methoxy and LYS200. Additionally, the O-3 feruloyl moiety shows π-π stacking interactions with TYR151. In comparison, the tetra-FSE **12** with the diisopropylidene bridges shows three hydrogen bonding between the O-3', O-4' and O-6' feruloyl aromatic OH with GLN63, ILE148 and ASP356, respectively. Its O-3 feruloyl is not involved in any type of interaction. As seen from this analysis, the ligand interactions diagrams for PSEs **12**, **14-16** reveals the order of interaction as: FSEs **16** > (four hydrogen bonds and one π stacking) > FSE **12** (three hydrogen bonds) ≈ FSE **15** (three hydrogen bonds) > FSE **14** (2 hydrogen bonds, one π stacking). Hydrogen bonds are stronger than π-π stacking interactions [22]. This trend is consistent with the inhibition activity values obtained from the *in vitro* experiments, which are in the order of: FSE **16** (98±1) > FSE **12** (54±4) ≈ FSE **15** (53±3) > FSE **14** (23±9).

Although both FSEs **12** and **16** have the same tetra-feruloyl substituents, their interactions with α-amylase and their *in vitro* inhibition values are very different (Figs. **5** and **3**). The differences are attributed to the absence of the diisopropylidene bridges in PSE **16,** which gives it greater steric flexibility, thus enabling it to adapt a better conformation (binding mode picture, supporting information). This confirmation allows the O-3 feruloyl moiety of FSE **16** to interact with the active site region unlike in the case of PSE **12** where the bridge imparts more rigidity and less steric freedom. Therefore, it can be concluded that the diisopropylidene ring plays an important role in the inhibition activity of the FSEs and this role is more pronounced in the case of α-amylase than in α-glucosidase. This is also clearly supported by the *in vitro* experimental results (Fig. **3**), docking experiments (Fig. **4**) and ligand inhibition diagrams (Fig. **5**).

2.6. Administration of FSE 12 to STZ-treated Diabetic Mice Shows Reduced PPHG in Comparison with Untreated Control Mice

FSE **12** was selected as the ideal candidate for *in vivo* efficacy studies based on its excellent selectivity: It showed a high 90±8% *in vitro* α-glucosidase inhibition activity and a desired lower α-amylase inhibition (54±4%). As discussed previously, this selectivity is desirable to reduce the GI side effects that accompany AGIs. The effect of FSE **12** on the postprandial hypoglycemic glucose (PPHG) levels as compared to the effect of acarbose in streptozotocin (STZ)-induced diabetic mice and. Here, either FSE **12** or acarbose were orally co-administered with starch to 4-hr fasted diabetic mice and the blood glucose was monitored for 2 hours post-administration (Fig. **8**). In all cases, the blood glucose levels peaked at 30 minutes after starch administration then kept decreasing. Both FSE **12** and acarbose significantly reduced the rise in blood glucose levels in comparison to the untreated group. In the group treated with FSE **12**, the blood glucose levels significantly decreased in comparison to the untreated group (Fig. **8**). Statistical tests on the data show that the acarbose treated group shows a significant decrease in blood glucose levels as compared to the untreated group at both 15 and 30 minutes after co-administration with starch. FSE **12** shows a statistically significant

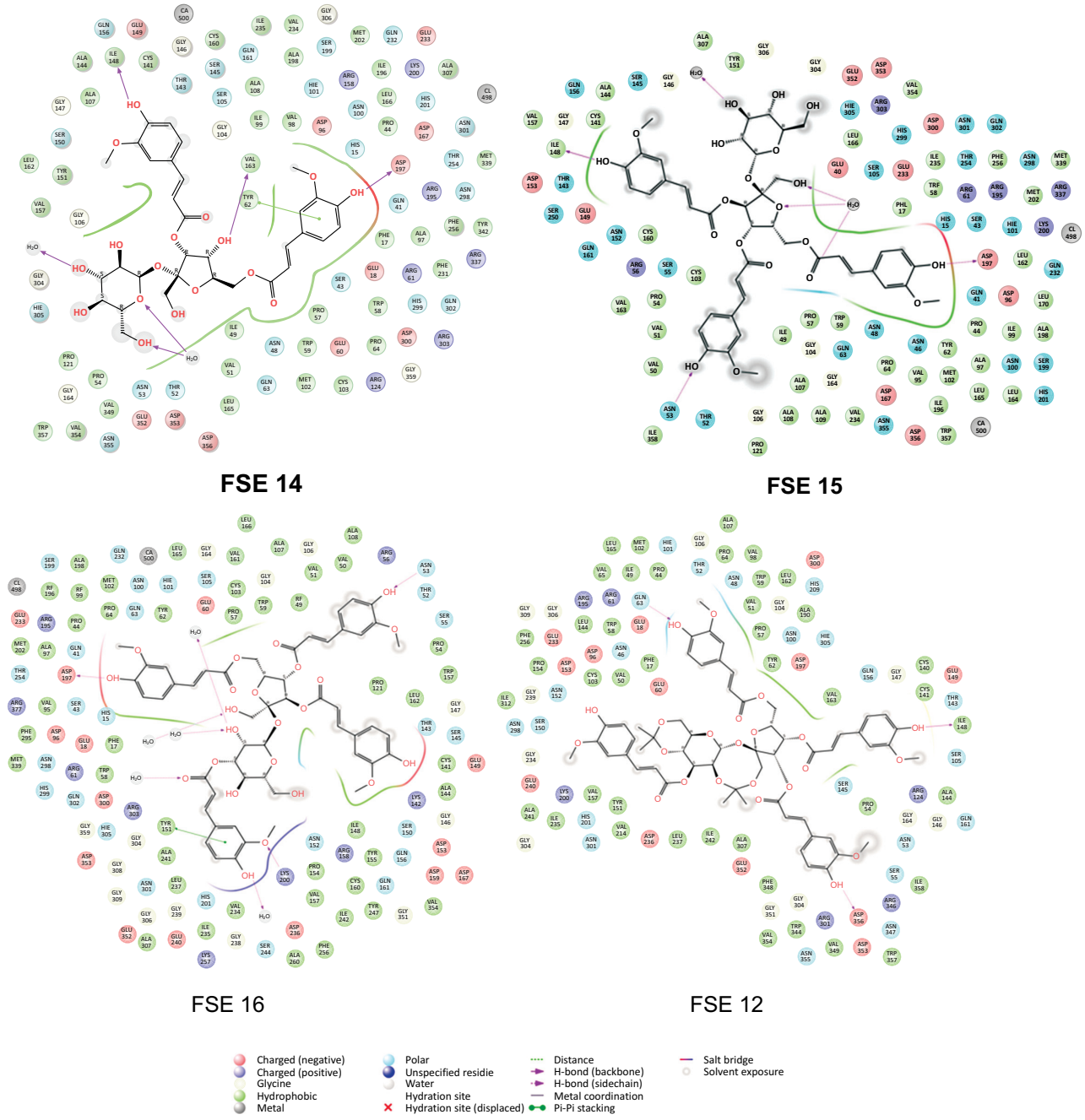

Fig. (7). Ligand Interaction Diagrams for the molecular docking top-scoring complexes between porcine pancreatic α-amylase and FSEs **12** and **14-16.** *(A higher resolution / colour version of this figure is available in the electronic copy of the article).*

decrease at 30 mins post co-administration. The results show that FSE **12** is just as effective as acarbose at controlling postprandial blood glucose at 30 mins and provide evidence that it acts as a potent AGI and anti-diabetic drug.

3. EXPERIMENTAL SECTION

3.1. Chemicals

α-Glucosidase, α-amylase from porcine pancreas, acarbose, 4-nitrophenyl α-D-glucopyranoside (PNPG), Dinitro Salicylic Acid (DNSA), DMSO, $NaHPO_4$, Na_2HPO_4 were purchased from Sigma Aldrich.

3.2. *In Vitro* α-glucosidase Inhibition Assay

α-Glucosidase inhibition was tested according to the previously reported method with minor modifications [22]. Briefly, 8 µl of DMSO containing FSE (50 µg/ml final concentration) was added to 115 µl of 0.1 M sodium phosphate buffer pH 7.0 in a 96 well microtitre plate. To this, 50 µl of yeast α-glucosidase enzyme so-

lution (0.5 U/ml in phosphate buffer) was added. The plate was incubated at 37 °C for 15 min. Next, 25 µl of 2.5 mM PNPG (4-nitrophenyl α -D-glucopyranoside) substrate solution (in phosphate buffer) was added to the wells. The microplate was incubated at 37 °C for another 15 minutes. Finally, the absorbance was measured at 405 nm using a microplate reader. The percentage inhibition was then calculated using the following formula:

$$\% \, inhibition = \frac{\Delta Abs_{control} - \Delta Abs_{sample}}{\Delta Abs_{control}} \, x \, 100$$

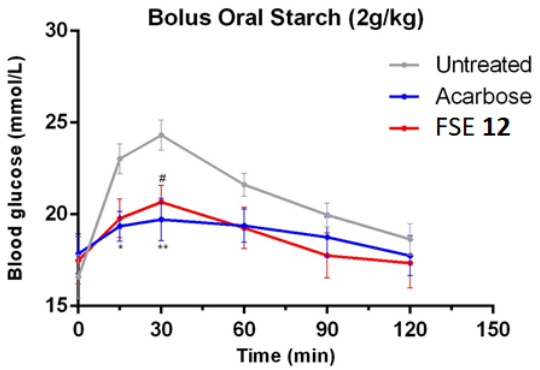

Fig. (8). Blood glucose response after bolus oral starch administration. FSE **12** and acarbose (10 mg/kg) were co-administered orally with starch (2g/kg). Values are expressed as mean ± SE (n=14). (* $p \leq 0.05$, ** $p \leq 0.01$: statistical significance for comparison of untreated with acarbose group; #$p \leq 0.05$: statistical significance for comparison of untreated with FSE **12** group). *(A higher resolution / colour version of this figure is available in the electronic copy of the article).*

3.3. *In Vitro* α-amylase Inhibition Assay

α-Amylase inhibition was tested using the previously reported method [22]. 50 µl of the FSEs in DMSO (final concentration 50 µg/ml) were added to test tubes. To these, 100 µ l of porcine pancreatic α -amylase (5 U/ml) and 460 µl of 0.05 M sodium phosphate buffer pH 6.8 were added. The tubes were incubated at 37 °C for 10 min. Following this, 450 µl of 0.5% starch solution was added and the tubes were incubated for a further 20 mins at 37 °C. Next, 500 µl of Dinitro Salicylic Acid (DNSA) reagent was added and the tubes were placed in a boiling water bath for 15 mins. The absorbance of the tubes was recorded at 540 nm and the % inhibition was calculated using the same formula as in the case of α-glucosidase,

$$\% \, inhibition = \frac{\Delta Abs_{control} - \Delta Abs_{sample}}{\Delta Abs_{control}} \, x \, 100$$

3.4. Calculation of IC_{50} and Statistical Analysis for Enzyme Inhibition

All measurements were performed in triplicates and the values are represented as mean ± std. deviation. The IC_{50} values for selected FSEs were calculated by plotting a dose-response curve using inhibition values for a range of concentrations for the selected FSEs (0-50 µg/ml) (data not shown) and performing regression analysis using Graphpad Prism software using the in-built function.

3.5. Molecular Docking of the PSEs 10-12 and 14-16 with α-glucosidase

A homology model for α-glucosidase from *Saccharomyces cerevisiae* was built by finding a suitable template using the 'BLAST' algorithm. Yeast isomaltase (PDB ID: 3A4A), which shared 72% sequence identity and 85% similarity with yeast α-glucosidase was used as a template to construct the homology model [18]. AutoDock was used for docking simulations and visualizations of the binding modes were done with Maestro. The receptor was prepared by first removing water molecules before adding Gasteiger charges and hydrogen atoms. To increase the flexibility of the docked ligands, the maximum number of rotatable bonds was chosen. The gridded binding site was chosen to be the site that houses the glucose molecule in the yeast isomaltase. The Lamarckian Genetic algorithm was chosen for the docking and a total of 100 binding modes were chosen.

3.6. Molecular Docking of the FSEs 12, 14-16 with α-amylase

Schrödinger's Maestro software was used to study the molecular interaction of the FSEs with porcine pancreatic α -amylase. The enzyme, porcine pancreatic α -amylase (PDB ID: 1OSE), was imported and the structure was processed using the Protein Preparation Wizard module. Following this, the receptor grid was generated based on the coordinates of the bound acarbose in the crystal structure, which was known as the primary binding site. Liu and co-workers have previously characterized two other binding sites within the enzyme [18], which are known as secondary binding sites and they are annotated here as SS1 and SS2. The Glide suite was used to perform the docking of the FSEs with the Extra Precision (XP) option. Water molecules that are 5 Å away from the primary binding site were retained during the docking. Besides, residues that possess bonds containing hydroxyl and thiol groups were considered to be flexible. On the other hand, single

bonds not having a specific chirality in the ligands are considered to be flexible as well.

3.7. Molecular Dynamics (MD) Simulations on FSEs 11-14

MD simulations were carried out for α-amylase using FSEs **11-14**. The lowest-energy docked poses for each FSEs **11-14** were used as initial structures for MD simulations. Structure preparation was done using LEaP module, while molecular dynamics production with ff99SB force field [24] was done using 'pmemd' module, both modules are part of AMBER 9.0 suite [25], TIP3P water molecules were added with the minimal distance between the complex and the edge of water box set as 5 Å. Counterions were added to maintain the neutrality of the system. Non-bonded cut-off was set to 12.0 Å. SHAKE algorithm [26], applied with all bonds involving hydrogen atoms restrained. After minimization and heating up from 10 to 300 K in 100 ps, production MD was carried out at 300 K, with a time step of 2.0 fs for 5 ns period, with complex conformation collected every 1 ps. For post-processing analysis and binding free energy calculation, all water molecules, counterions, and periodic boundary information were removed from the trajectory. A single-trajectory approach was used for all binding free energy calculations. Five hundred regular snapshots were used for solvated interaction energy (SIE) using sietraj [27, 28] to calculate binding free energy.

3.8. Experimental Animals

Male mice strain C57BL/6J was used for the experiments. All animals were housed individually in light (12 h on/12 h off) and temperature-controlled room with pelleted food and water available ad libitum. They were split into three groups: FSE, acarbose, and untreated control. After an adjustment period of 1 week, they were injected with STZ for induction of diabetes. All procedures were approved by IACUC (protocol number 140905).

3.8.1. STZ Injection

Diabetes was induced in mice by intraperitoneal STZ injection [29]. The mice were injected with 50 mg/kg dose for 5 consecutive days [30]. Mice displaying polyuria, weight loss and those having fasting blood glucose greater than 12 mM (250 mg/dL) were considered to be diabetic and were used for further experiments.

3.8.2. In Vivo Study for Hypoglycemic Effects of PSE 12

The mice were fasted for 8 hours but were given free access to water. Following this, the mice were administered FSE **12** or acarbose (10 mg/kg body weight) mixed with starch (2 g/kg) by oral gavage. Control mice received only the oral starch load. The blood glucose was measured at 'time 0' before administration and following the co-administration of starch and the drugs, the blood glucose was measured at 15, 30, 60, 90, and 120 minutes time intervals [31].

3.8.3. Statistical Analysis

Statistical analysis was performed using Graphpad Prism software. All measurements were made in triplicates for *in vitro* studies with values represented as means ± standard deviation and the data set evaluated by one-way ANOVA with the statistical significance set at $p<0.05$. For *in vivo* studies, the values represented in the graphs are mean ± standard error. The data set was evaluated by two-way ANOVA followed by Tukey's post hoc test with the statistical significance set at $p<0.05$.

3.9. Synthesis of FSEs 5, 9 and 13

The synthesis of FSEs **1-16** was reported in our previous work except for FSEs **5**, **9** and **13** [19-21].

3.9.1. Reagents and Methods

All commercial materials used in this work were obtained from Sigma-Aldrich, Acros, Merck and Fisher scientific and were used as received. IR spectra were recorded using KBr on a DIGILAB FTIR-FTS 3100 spectrometer. Routine ^{1}H NMR spectra were recorded at 300 MHz on a Bruker Avance DPX 300 spectrometer. ^{1}H NMR multiplicities were designated as singlet (s), doublet (d), doublet of doublet (dd), doublet of doublet of doublet (ddd), triplet (t), quartet (q), multiplet (m), broad (br), apparent (app). ^{13}C NMR spectra were measured at 75.47 MHz on a Bruker Avance DPX 300 spectrometer. Routine mass spectra were recorded on LCQ mass spectrometer from Thermo, using ESI positive mode. HR mass spectra were recorded on Finnigan MAT95XL-T spectrometer using ESI positive mode. Flash chromatography and column chromatography were carried out using Merck silica gel 60 230-400 mesh. The products on the TLC plate were visualized under UV light (254 nm) or by using a solution of 5% H_2SO_4 in EtOH (v/v).

3.9.2. Synthesis of 6'-O-acetylferuloyl sucrose 5

A solution of FSE **1** (0.1 g, 0.2 mmol) in 60% aq. AcOH (6.4 mL) was stirred at 80 °C for 20 min (TLC; 3:2 EtOAc-CH_2Cl_2). The reaction solution was co-distilled with toluene (3 x 100 mL) then evaporated to dryness under reduced pressure. FSE **5** was obtained after recrystallization from EtOAc as a white solid

(0.09 g, 86% yield). R_f = 0.08 (9:1 EtOAc-MeOH); m.p.: 168-170 °C; FT-IR (KBr) ν_{max}: 3324, 2927, 1754, 1712, 1687, 1640, 1600, 1547, 1514, 1467, 1421, 1372, 1332, 1262, 1218, 1187, 1158, 1123, 1062, 1032, 995, 917, 902, 834 cm^{-1}; ^1H NMR (300 MHz, CD_3OD): δ 3.33 (m, 1H, H-4), 3.37-3.43 (m, 1H, H-2), 3.64 (m, 2H, H-1′a, H-1′b), 3.69-3.75 (dd, 2H, H-6a, H-3), 3.84-3.90 (m, 2H, H-5, H-6b), 3.99-4.01 (m, 1H, H-5′), 4.06-4.14 (m, 2H, H-3′, H-4′), 4.42-4.52 (m, 2H, H-6′b, H-6′a), 5.39 (d, 1H, *J* = 3.6 Hz, H-1); *trans*-*p*-feruloyl units: δ 2.27 (s, 3H, H-11″); 3.87 (s, 3H, -OC*H*$_3$), 6.57 (d, 1H, *J* = 15.9 Hz, H-8″), 7.05-7.09 (m, 1H, H-6″), 7.19-7.24 (m, 1H, H-5″), 7.32-7.34 (m, 1H, H-2″), 7.71 (d, 1H, *J* = 15.9 Hz, H-7″); ^{13}C NMR (75.48 MHz, CD_3OD): δ 62.6 (C-6), 63.9 (C-1′), 67.0 (C-6′), 71.6 (C-4), 73.4 (C-2), 74.3 (C-5), 74.8 (C-3), 76.9 (C-4′), 79.0 (C-3′), 80.8 (C-5′), 93.6 (C-1), 105.7 (C-2′); *trans*-*p*-feruloyl units: 20.5 (C-11″), 56.6 (-O*C*H$_3$), 112.8 (C-2″), 119.1 (C-8″), 122.4 (C-5″), 124.4 (C-6″), 134.8 (C-1″), 143.1 (C-3″), 146.0 (C-7″), 153.1 (C-4″), 168.5 (C-9″), 170.6 (C-10″); ESI-Mass (positive mode): *m/z* 583.10 $[M + Na]^+$, calcd. 583.17 for $C_{24}H_{32}O_{15}Na$; HR-ESI-MS (positive mode): found *m/z* 583.1628 $[M + Na]^+$, calcd 583.1633 for $C_{24}H_{32}O_{15}Na$.

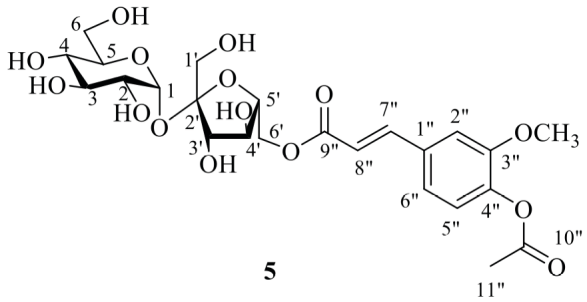

5

3.9.3. Synthesis of 6'-O-(4-tert-butyldimethylsiloxy-3-methoxycinnamoyl)-2,1'-di-O-isopropylidene sucrose 18

A solution of *p-tert*-butyldimethylsilyloxy-3-methoxycinnamic acid (437 mg, 1.42 mmol), oxalyl chloride (132 µL, 1.54 mmol) and DMF (18.3 µL, 0.237 mmol) in CH_2Cl_2 (3.0 ml) was stirred for 2 hours before the addition of a solution of 2,1':4,6-di-*O*-isopropylidene sucrose **17** (500 mg, 1.18 mmol) in pyridine (286.2 µL, 3.55 mmol) and CH_2Cl_2 (2.0 ml). The reaction mixture was left to stir for 12 hours then evaporated to dryness. The crude product obtained was purified by column chromatography using a gradient (starting from 2:1 Hexane/EtOAc and slowly increase EtOAc) to give compound **18** in 43 % yield. m.p.: 88.6-89.8 °C; ^1H NMR (300 MHz, $CDCl_3$): TBS on OTBS-feruloyl group: δ 0.00 (s, 6H, $(CH_3)_2Si$), 0.83 (s, 9H, $(CH_3)_3CSi$); isopropylidene rings: δ 1.28-1.34 (m, 12H, 2 x $(CH_3)_2C$); methoxy and sucrose unit: δ 3.32-3.45 (m, 2H, H-5, H-1'), 3.54-3.60 (m, 3H, H-2, H-6, H-1'), 3.65 (s, 3H, 3 x OCH_3), 3.74-3.79 (m, 3H, H-4, H-6, H-3'), 3.92-4.17 (m, 4H, H-3, H-4', H-5', H-6a'), 4.41 (m, 1H, H-6b'), 6.04 (s, 1H, H-1); *trans*-alkenyl and aromatic protons: δ 6.17 (d, 1H, *J* = 18 Hz, H-8″), 6.66 (d, 1H, *J* = 9 Hz, H-5″), 6.84 (m, 2H, H-2″. H-6″), 7.46 (d, 1H, *J* = 15 Hz, H-7″); ^{13}C NMR (75.5 MHz, $CDCl_3$): δ -3.60, -3.57, 11.0, 18.5, 19.0, 23.8, 25.2, 25.6, 25.7, 29.0, 29.3, 29.7, 37.8, 38.0, 38.1, 53.5, 55.4, 62.1, 64.2, 64.9, 65.9, 70.9, 71.3, 71.6, 79.5, 91.4, 99.7, 101.5, 104.5, 110.8, 115.4, 121.0, 122.4, 128.3, 145.2, 147.5, 151.2, 166.7, 171.1; HR-MS (ESI-positive mode): found *m*/z 713.3122 $[M+H]^+$, calcd. for $C_{34}H_{53}O_{14}Si$ 713.3160.

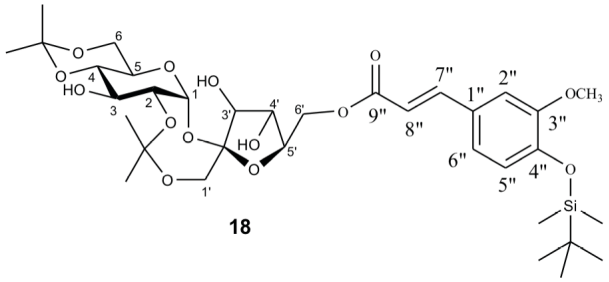

18

3.9.4. Synthesis of FSE 9: 6'-O-feruloyl-2,1':4,6-di-O-isopropylidene Sucrose

Compound **18** (200 mg, 0.281 mmol) was dissolved in pyridine (1.0 ml) and stirred at room temperature. 1.56 M $3HF{\cdot}NEt_3$ (540 µL, 0.842 mmol) and NEt_3 (78.4 µL, 0.562 mmol) were added to the reaction solution, which was then left to stir for 12 hours. Upon completion, pyridine was removed under vacuum. The crude product was then subjected to purification with column chromatography using 2:1 EtOAc/Hexane as eluent to give **9** as white solid in 83% yield. Comparison with reported values in literature[21] confirmed the formation of **9**.

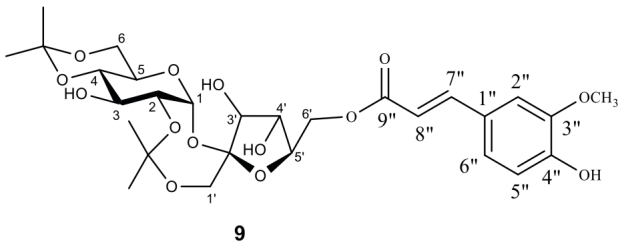

9

3.9.5. Synthesis of PSE 13: 6'-O-feruloyl Sucrose

To a stirred suspension of FSE **5** (0.2 g, 0.3 mmol) in 95% EtOH (13 mL), piperidine (63.5 µL, 54.7 mg, 0.6 mmol) was added at room temperature whereupon the solution turned yellow. The stirring was continued for 7 hours (TLC, 9:1 EtOAc-MeOH). The mixture was

then quenched with AcOH and evaporated to form a syrup. It was subjected to silica gel column chromatography using a gradient of CH_2Cl_2-EtOAc-MeOH as eluent to give FSE **13** as a white solid (0.12 g, 72% yield). R_f = 0.08 (9:1 EtOAc-MeOH); m.p.: 133-135 ^oC; FT-IR (KBr) ν_{max}: 3443, 3360, 2958, 2932, 2890, 1726, 1691, 1637, 1603, 1517, 1467, 1433, 1373, 1322, 1293, 1279, 1259, 1181, 1134, 1102, 1074, 1027, 999, 953, 933, 878, 838, 680 cm^{-1}; ^1H NMR (300 MHz, CD_3OD): δ 3.38 (d, 1H, *J* = 9.6 Hz, H-4), 3.44 (dd, 1H, *J* = 3.6 Hz, 9.9 Hz, H-2), 3.50-3.69 (m, 2H, H-1′a, H-1′b), 3.71-3.77 (m, 2H, H-6a, H-3), 3.85-3.96 (m, 2H, H-5, H-6b), 4.04-4.08 (m, 2H, H-5′, H-4′), 4.14 (m, 1H, H- 3′), 4.44-4.50 (m, 2H, H-6′b, H-6′a), 5.41 (d, 1H, *J* = 3.6 Hz, H-1); *trans-p*-feruloyl units: δ 3.88 (s, 3H, -OC*H*$_3$), 6.37 (d, 1H, *J* = 15.9 Hz, H-8″), 6.81 (d, 1H, *J* = 8.1 Hz, H-6″), 7.06 (d, 1H, *J* = 8.4 Hz, H-5″), 7.16 (br s, 1H, H-2″), 7.63 (d, 1H, *J* = 15.9 Hz, H-7″); ^{13}C NMR (75.48 MHz, CD_3OD): δ 62.5 (C-6), 63.9 (C-1′), 66.8 (C-6′), 71.5 (C-4), 73.3 (C-2), 74.3 (C-5), 74.7 (C-3), 76.9 (C-4′), 79.1 (C-3′), 80.7 (C-5′), 93.5 (C-1), 105.5 (C-2′); *trans-p*-feruloyl units: δ 56.5 (-O*C*H$_3$), 111.8 (C-2″), 115.2 (C-8″), 116.5 (C-5″), 124.2 (C-6″), 127.7 (C-1″), 147.2 (C-7″), 149.4 (C-3″), 150.7 (C-4″), 169.2 (C-9″); ESI-Mass (positive mode): found *m/z* 541.09 $[M + Na]^+$, calcd 541.16 for $C_{22}H_{30}O_{14}Na$; HR-ESI-MS (positive mode): found *m/z* 541.1516 $[M + Na]^+$, calcd 541.1528 for $C_{22}H_{30}O_{14}Na$.

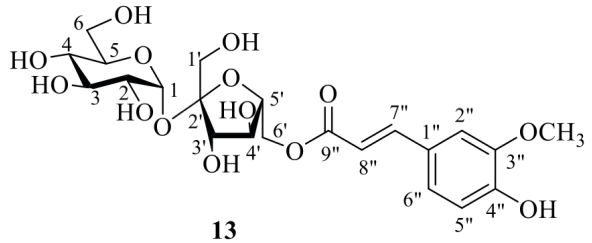

13

CONCLUSION

The inhibition of α-glucosidase and α-amylase by 16 feruloyl sucrose esters (FSEs) was investigated to establish an accurate structure-activity relationship with the overarching aim of developing selective alpha-glucosidase inhibitors (AGIs) to circumvent the gastrointestinal side effects of current AGIs. The FSEs structural features, including the number of feruloyl moieties, aromatic OH groups and the diisopropylidene bridges, greatly impact the inhibition activities of both enzymes. Consequently, the desired selective high inhibition of α-glucosidase and low inhibition of α-amylase is achievable with proper control of these structural features. There was a striking agreement between the *in vitro* experiments and *in silico* studies where binding modes, ligand interaction diagrams and free energy of binding successfully explained the differences in the *in vitro* studies. The inhibition activities of both α-glucosidase and α-amylase increased with the increase in the number of feruloyl moieties and aromatic OH groups. However, the absence of diisopropylidene bridges increases the inhibition in α-glucosidase and its presence decreases the inhibition of α-amylase. FSE **12** was as effective as acarbose at controlling postprandial blood glucose at 30 mins in STZ diabetic mice. The promising inhibition results and the ability to achieve selective inhibition should be further explored to develop FSEs as AGI candidates with minimum side effects for the treatment of type 2 diabetes.

AUTHORS' CONTRIBUTIONS

Zaher Judeh supervised the synthetic work, Yusuf Ali supervised the *in vivo* study and Dawei Zhang supervised the molecular modelling studies. Surabhi Devraj performed the *in vitro*, *in vivo*, and *in silico* studies. Yew Mun Yip performed part of the *in silico* studies. Parthasarathi Panda, Pooi Wen Kathy Wong, and Li Lin Ong synthesized the compounds.

LIST OF ABBREVIATIONS

AGIs	=	Alpha Glucosidase Inhibitors
BE	=	Binding Energy
FSEs	=	Feruloyl Sucrose Esters
IACUC	=	Institutional Animal Care and Use Committee
LID	=	Ligand Interaction Diagram
MD	=	Molecular Dynamics
PPHG	=	Post Prandial Hyperglycemia
PSEs	=	Phenylpropanoid Sucrose Esters
SAR	=	Structure Activity Relationship
SS1	=	Secondary Site 1
SS2	=	Secondary Site 2
STZ	=	Streptozotocin

ETHICS APPROVAL AND CONSENT TO PARTICIPATE

All procedures were approved by IACUC of Nanyang Technological University Singapore, (protocol number 140905), Singapore.

HUMAN AND ANIMAL RIGHTS

No humans were used in this study. All animal studies were carried out in a National Advisory Committee

for Laboratory Animal Research (NACLAR) facility guided by the US National Research Council's.

CONSENT FOR PUBLICATION

Not applicable.

AVAILABILITY OF DATA AND MATERIALS

Not applicable.

FUNDING

This work has been funded by the Nanyang Technological University, College of Engineering Start Up Grant. In addition, this work was also supported by the Singapore Ministry of Education, Tier 1 grant (2019-T1-001-059) (YA).

CONFLICT OF INTEREST

The authors declare no conflict of interest, financial or otherwise.

ACKNOWLEDGEMENTS

All the authors are thankful for the financial support provided by the Nanyang Technological University and College of Engineering Start Up Grant, and Singapore Ministry of education.

SUPPLEMENTARY MATERIAL

The supplementary material is available with the article on the publisher's website.

REFERENCES

[1] IDF Diabetes Atlas. International diabetes federation: Brussels, **2019**. Available from: https://www.diabetesatlas.org/ [Accessed 8th June 2020]

[2] Kruger, D.F. Exploring the pharmacotherapeutic options for treating type 2 diabetes. *Diabetes Educ.,* **2008**, *34*(3)(Suppl. 3), 60S-65S. http://dx.doi.org/10.1177/0145721708319234 PMID: 18525066

[3] *World Health Organisation-fact sheet- diabetes,* Available from: https://www.who.int/news-room/fact-sheets/detail/diabetes [Accessed 8th June 2020]

[4] Akkati, S.; Sam, K.G.; Tungha, G. Emergence of promising therapies in diabetes mellitus. *J. Clin. Pharmacol.,* **2011**, *51*(6), 796-804. http://dx.doi.org/10.1177/0091270010376972 PMID: 20705952

[5] Levetan, C. Oral antidiabetic agents in type 2 diabetes. *Curr. Med. Res. Opin.,* **2007**, *23*(4), 945-952. http://dx.doi.org/10.1185/030079907X178766 PMID: 17407651

[6] Kumar, R.V.; Sinha, V.R. Newer insights into the drug delivery approaches of α -glucosidase inhibitors. *Expert Opin. Drug Deliv.,* **2012**, *9*(4), 403-416. http://dx.doi.org/10.1517/17425247.2012.663080 PMID: 22364261

[7] Hanefeld, M.; Schaper, F. The role of alpha-glucosidase inhibitors (acarbose). *Pharmacotherapy of diabetes: New Developments,* **2007**, 143-152.

[8] Zhang, W.; Kim, D.; Philip, E.; Miyan, Z.; Barykina, I.; Schmidt, B.; Stein, H. A multinational, observational study to investigate the efficacy, safety and tolerability of acarbose as add-on or monotherapy in a range of patients: The Gluco VIP study. *Clin. Drug Investig.,* **2013**, *33*(4), 263-274. http://dx.doi.org/10.1007/s40261-013-0063-3 PMID: 23435929

[9] Derosa, G.; Maffioli, P. α-Glucosidase inhibitors and their use in clinical practice. *Arch. Med. Sci.,* **2012**, *8*(5), 899-906. http://dx.doi.org/10.5114/aoms.2012.31621 PMID: 23185202

[10] Kelley, D.E.; Bidot, P.; Freedman, Z.; Haag, B.; Podlecki, D.; Rendell, M.; Schimel, D.; Weiss, S.; Taylor, T.; Krol, A.; Magner, J. Efficacy and safety of acarbose in insulin-treated patients with type 2 diabetes. *Diabetes Care,* **1998**, *21*(12), 2056-2061. http://dx.doi.org/10.2337/diacare.21.12.2056 PMID: 9839094

[11] Cardullo, N.; Muccilli, V.; Pulvirenti, L.; Cornu, A.; Pouységu, L.; Deffieux, D.; Quideau, S.; Tringali, C. C-glucosidic ellagitannins and galloylated glucoses as potential functional food ingredients with anti-diabetic properties: A study of α -glucosidase and α -amylase inhibition. *Food Chem.,* **2020**, *313*, 126099. http://dx.doi.org/10.1016/j.foodchem.2019.126099 PMID: 31927321

[12] Costamagna, M.S.; Zampini, I.C.; Alberto, M.R.; Cuello, S.; Torres, S.; Pérez, J.; Quispe, C.; Schmeda-Hirschmann, G.; Isla, M.I. Polyphenols rich fraction from Geoffroea decorticans fruits flour affects key enzymes involved in metabolic syndrome, oxidative stress and inflammatory process. *Food Chem.,* **2016**, *190*, 392-402. http://dx.doi.org/10.1016/j.foodchem.2015.05.068 PMID: 26212988

[13] Ranilla, L.G.; Kwon, Y-I.; Apostolidis, E.; Shetty, K. Phenolic compounds, antioxidant activity and *in vitro* inhibitory potential against key enzymes relevant for hyperglycemia and hypertension of commonly used medicinal plants, herbs and spices in Latin America. *Bioresour. Technol.,* **2010**, *101*(12), 4676-4689. http://dx.doi.org/10.1016/j.biortech.2010.01.093 PMID: 20185303

[14] Guo, Z-H.; Huang, J.; Wan, G-S.; Huo, X-L.; Gao, H-Y. New inhibitors of α -glucosidase in *Salacia hainanensis* Chun et How. *J. Nat. Med.,* **2013**, *67*(4), 844-849. http://dx.doi.org/10.1007/s11418-013-0744-5 PMID: 23361306

[15] Phan, M.A.T.; Wang, J.; Tang, J.; Lee, Y.Z.; Ng, K. Evaluation of α -glucosidase inhibition potential of some flavonoids from *epimedium brevicornum. Lebensm. Wiss. Technol.,* **2013**, *53*(2), 492-498. http://dx.doi.org/10.1016/j.lwt.2013.04.002

[16] Panda, P.; Appalashetti, M.; Judeh, Z.M.A. Phenylpropanoid sucrose esters: Plant-derived natural products as potential leads for new therapeutics. *Curr. Med. Chem.,* **2011**, *18*(21), 3234-3251. http://dx.doi.org/10.2174/092986711796391589 PMID: 21671860

[17] Fan, P.; Terrier, L.; Hay, A-E.; Marston, A.; Hostettmann, K. Antioxidant and enzyme inhibition activities and chemi-

cal profiles of *Polygonum sachalinensis* F.Schmidt ex Maxim (Polygonaceae). *Fitoterapia,* **2010**, *81*(2), 124-131. http://dx.doi.org/10.1016/j.fitote.2009.08.019 PMID: 19698767

[18] Liu, T.; Yip, Y.M.; Song, L.; Feng, S.; Liu, Y.; Lai, F.; Zhang, D.; Huang, D. Inhibiting enzymatic starch digestion by the phenolic compound diboside A: A mechanistic and *in silico* study. *Food Res. Int.,* **2013**, *54*(1), 595-600. http://dx.doi.org/10.1016/j.foodres.2013.07.062

[19] Panda, P.; Appalashetti, M.; Natarajan, M.; Chan-Park, M.B.; Venkatraman, S.S.; Judeh, Z.M. Synthesis and antitumor activity of lapathoside D and its analogs. *Eur. J. Med. Chem.,* **2012**, *53*, 1-12. http://dx.doi.org/10.1016/j.ejmech.2012.02.032 PMID: 22542106

[20] Panda, P.; Appalashetti, M.; Natarajan, M.; Mary, C-P.; Venkatraman, S.S.; Judeh, Z.M. Synthesis and antiproliferative activity of helonioside A, 3′,4′,6′-tri-O-feruloylsucrose, lapathoside C and their analogs. *Eur. J. Med. Chem.,* **2012**, *58*, 418-430. http://dx.doi.org/10.1016/j.ejmech.2012.10.034 PMID: 23153813

[21] Panda, P. *Synthesis and anticancer activity of phenylpropanoid sucrose esters.* Doctoral dissertation*,* Nanyang Technological University: Singapore, **2011**.

[22] Yan, J.; Zhang, G.; Pan, J.; Wang, Y. α-Glucosidase inhibition by luteolin: Kinetics, interaction and molecular docking. *Int. J. Biol. Macromol.,* **2014**, *64*, 213-223. http://dx.doi.org/10.1016/j.ijbiomac.2013.12.007 PMID: 24333230

[23] Steed, J.W.; Atwood, J.L. Supramolecular chemistry.John Wiley & Sons Ltd.: London, **2009**. http://dx.doi.org/10.1002/9780470740880

[24] Hornak, V.; Abel, R.; Okur, A.; Strockbine, B.; Roitberg, A.; Simmerling, C. Comparison of multiple amber force fields and development of improved protein backbone parameters. *Proteins Struct. Funct. Bioinform.,* **2006**, *65*, 712-725.

[25] Case, D.A.; Darden, T.A.; Cheatham, T.E., III; Simmerling, C.L.; Wang, J.; Duke, R.E.; Luo, R.; Merz, K.M.; Pearlman, D.A.; Crowley, M.; Walker, R.C.; Zhang, W.; Wang, B.; Hayik, S.; Roitberg, A.; Seabra, G.; Wong, K.F.; Paesani, F.; Wu, X.; Brozell, S.; Tsui, V.; Gohlke, H.; P. A. K. Amber, L. **2006**.

[26] Ryckaert, J-P.; Ciccotti, G.; Berendsen, H.J.C. Numerical integration of the cartesian equations of motion of a system with constraints: Molecular dynamics of n-alkanes. *J. Comput. Phys.,* **1977**, *23*, 327-341. http://dx.doi.org/10.1016/0021-9991(77)90098-5

[27] Naïm, M.; Bhat, S.; Rankin, K.N.; Dennis, S.; Chowdhury, S.F.; Siddiqi, I.; Drabik, P.; Sulea, T.; Bayly, C.I.; Jakalian, A.; Purisima, E.O. Solvated interaction energy (SIE) for scoring protein-ligand binding affinities. 1. Exploring the parameter space. *J. Chem. Inf. Model.,* **2007**, *47*(1), 122-133. http://dx.doi.org/10.1021/ci600406v PMID: 17238257

[28] Cui, Q.; Sulea, T.; Schrag, J.D.; Munger, C.; Hung, M.N.; Naïm, M.; Cygler, M.; Purisima, E.O. Molecular dynamics-solvated interaction energy studies of protein-protein interactions: The MP1-p14 scaffolding complex. *J. Mol. Biol.,* **2008**, *379*(4), 787-802. http://dx.doi.org/10.1016/j.jmb.2008.04.035 PMID: 18479705

[29] Wu, K. K.; Huan, Y. Streptozotocin-induced diabetic models in mice and rats. *Curr. Protoc. Pharmacol.,* **2008**, *40*(SUPPL.), 1-14. http://dx.doi.org/10.1002/0471141755.ph0547s40

[30] Brosius, F. Low-dose streptozotocin induction protocol (mouse) summary: Reagents and materials: Reagent preparation: Protocol. **2003**, 4-6.

[31] Park, M.H.; Ju, J.W.; Park, M.J.; Han, J.S. Daidzein inhibits carbohydrate digestive enzymes *in vitro* and alleviates postprandial hyperglycemia in diabetic mice. *Eur. J. Pharmacol.,* **2013**, *712*(1-3), 48-52. http://dx.doi.org/10.1016/j.ejphar.2013.04.047 PMID: 23669248